



Optimization of anti-*Trypanosoma cruzi* oxadiazoles leads to identification of compounds with efficacy in infected mice

José Maurício dos Santos Filho^{a,*}, Diogo Rodrigo M. Moreira^{b,e}, Carlos Alberto de Simone^c, Rafaela Salgado Ferreira^{d,†}, James H. McKerrow^d, Cássio Santana Meira^e, Elisalva Teixeira Guimarães^{e,f}, Milena Botelho Pereira Soares^{e,g}

^a Departamento de Engenharia Química, Centro de Tecnologia e Geociências, Universidade Federal de Pernambuco, CEP 50740-521, Recife, PE, Brazil

^b Departamento de Ciências Farmacêuticas, Centro de Ciências da Saúde, Universidade Federal de Pernambuco, 50740-520, Recife, PE, Brazil

^c Departamento de Física e Informática, Instituto de Física, Universidade de São Paulo, CEP 13560-970, São Carlos, SP, Brazil

^d Sandler Center for Drug Discovery in Parasitic Diseases, University of California, San Francisco, CA 94158, USA

^e Centro de Pesquisas Gonçalo Moniz, Fundação Oswaldo Cruz, CEP 40296-750, Salvador, BA, Brazil

^f Departamento de Ciências da Vida, Universidade Estadual da Bahia, CEP 41150-000, Salvador, BA, Brazil

^g Centro de Biotecnologia e Terapia celular, Hospital São Rafael, CEP 41253-190, Salvador, BA, Brazil

ARTICLE INFO

Article history:

Received 6 July 2012

Revised 16 August 2012

Accepted 23 August 2012

Available online 31 August 2012

Keywords:

Chagas disease

Trypanosoma cruzi

Cruzain

Oxadiazoles

Hydrazones

Bioisosterism

ABSTRACT

We recently showed that oxadiazoles have anti-*Trypanosoma cruzi* activity at micromolar concentrations. These compounds are easy to synthesize and show a number of clear and interpretable structure–activity relationships (SAR), features that make them attractive to pursue potency enhancement. We present here the structural design, synthesis, and anti-*T. cruzi* evaluation of new oxadiazoles denoted **5a–h** and **6a–h**. The design of these compounds was based on a previous model of computational docking of oxadiazoles on the *T. cruzi* protease cruzain. We tested the ability of these compounds to inhibit catalytic activity of cruzain, but we found no correlation between the enzyme inhibition and the antiparasitic activity of the compounds. However, we found reliable SAR data when we tested these compounds against the whole parasite. While none of these oxadiazoles showed toxicity for mammalian cells, oxadiazoles **6c** (fluorine), **6d** (chlorine), and **6e** (bromine) reduced epimastigote proliferation and were cidal for trypomastigotes of *T. cruzi* Y strain. Oxadiazoles **6c** and **6d** have IC₅₀ of 9.5 ± 2.8 and 3.5 ± 1.8 μM for trypomastigotes, while Benznidazole, which is the currently used drug for Chagas disease treatment, showed an IC₅₀ of 11.3 ± 2.8 μM. Compounds **6c** and **6d** impair trypomastigote development and invasion in macrophages, and also induce ultrastructural alterations in trypomastigotes. Finally, compound **6d** given orally at 50 mg/kg substantially reduces the parasitemia in *T. cruzi*-infected BALB/c mice. Our drug design resulted in potency enhancement of oxadiazoles as anti-Chagas disease agents, and culminated with the identification of oxadiazole **6d**, a trypanosomicidal compound in an animal model of infection.

© 2012 Elsevier Ltd. All rights reserved.

1. Introduction

It is estimated that 10% of the whole Latin America population is suffering from American trypanosomiasis or Chagas disease, caused by the intracellular protozoan *Trypanosoma cruzi*.^{1,2} This situation is alarming because there are no vaccines available and the current treatment, which is only based on benznidazole (Bdz), suffers limitations of efficacy and toxicity.^{3,4}

The *T. cruzi* cysteine-protease cruzain is an important drug target because it is expressed in all stages of the parasite life cycle and play key roles as a virulence factor.^{5–8} An important proof-concept

of cruzain as a drug target is that its inhibitors efficiently eradicate parasites in host-cells and substantially reduce parasitemia in different animal models of infection.^{9,10} The current status of cruzain inhibitor research is quite promising because some of these lead compounds are nonpeptidic and quite similar to drug-like compounds, a step that is important for successful drug development.^{10–12} Therefore, the identification or structural optimization of cruzain inhibitors is a promising avenue for Chagas disease chemotherapy.

There is a substantial number of papers reporting oxadiazoles as anti-parasitics. Oxadiazoles are frequently explored as bioisosters of ester and amide functionalities. From this point of view, oxadiazoles are considered potential cysteine protease inhibitors because they are similar to peptide bonds.^{13–15} There are reports showing that oxadiazoles are potent inhibitors versus cruzain of *T. cruzi* and the cathepsin-L-like cysteine protease of *Leishmania*

* Corresponding author. Tel.: +55 81 21267288; fax: + 55 81 21267278.

E-mail address: mauricio_santosfilho@yahoo.com.br (J.M. dos Santos Filho).

† Present address: Departamento de Bioquímica e Imunologia, Universidade Federal de Minas Gerais, Belo Horizonte, MG, Brazil.

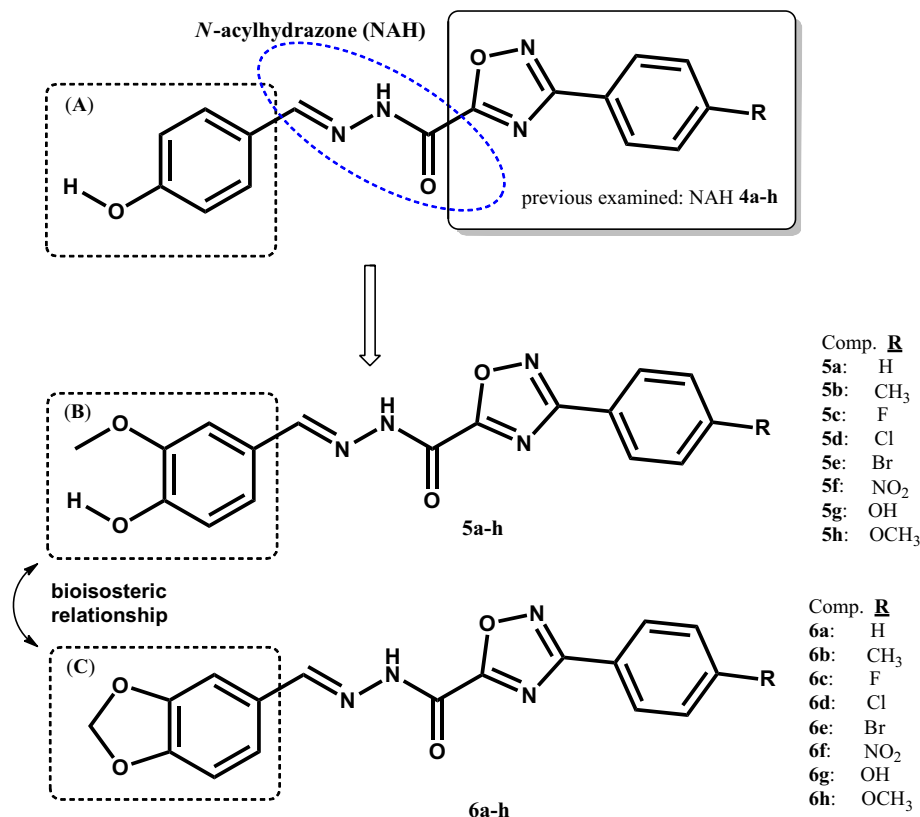


Figure 1. Structural design of oxadiazoles **5a-h** and **6a-h** as trypanocidal compounds.

mexicana.^{16–20} In light of these findings, we found reasonable to explore oxadiazoles as anti-*T. cruzi* agents. In 2009, we reported a congener series of *N*-acylhydrazone 1,2,4-oxadiazoles, denoted **4a-h**, exhibiting toxicity for trypomastigotes of *T. cruzi* Y strain.²¹ The oxadiazoles **4a-h** showed minimal toxicity for mouse splenocytes and a clear set of structure–activity relationships. A computational model of docking suggested oxadiazoles **4a-h** might be cruzain ligands. This model also suggested that the 4-hydroxyphenyl group near to the *N*-acylhydrazone is probably oriented in a region of cruzain structure which is also the binding site for highly-potent cruzain inhibitors.¹² Based on this binding model, we thought that structural modifications on 4-hydroxyphenyl might lead to potency enhancement (Fig. 1).

The functional activity of oxadiazole **4a-h** as trypanosomicidal compounds led us to explore potency enhancement by molecular modification. For this study, we synthesized oxadiazoles **5a-h** and **6a-h**, composed of the 3-aryl-1,2,4-oxadiazole-5-carbohydrazides of the previously identified anti-*T. cruzi* oxadiazoles **4a-h** with a replacement of 4-hydroxyphenyl group by 4-hydroxy-3-methoxyphenyl for **5a-h** and 1,3-benzodioxole for **6a-h**. These chemical replacements were selected due to the analogy between these chemical groups (Fig. 1).^{22–24} Enhancement of anti-*T. cruzi* activity in parasite cells was indeed achieved for oxadiazoles **6a-h**, furthermore these oxadiazoles impaired trypomastigote development and invasion into host-cells, and mice orally treated with oxadiazole **6d** had a substantial reduction of parasitemia.

2. Results and discussion

2.1. Chemistry

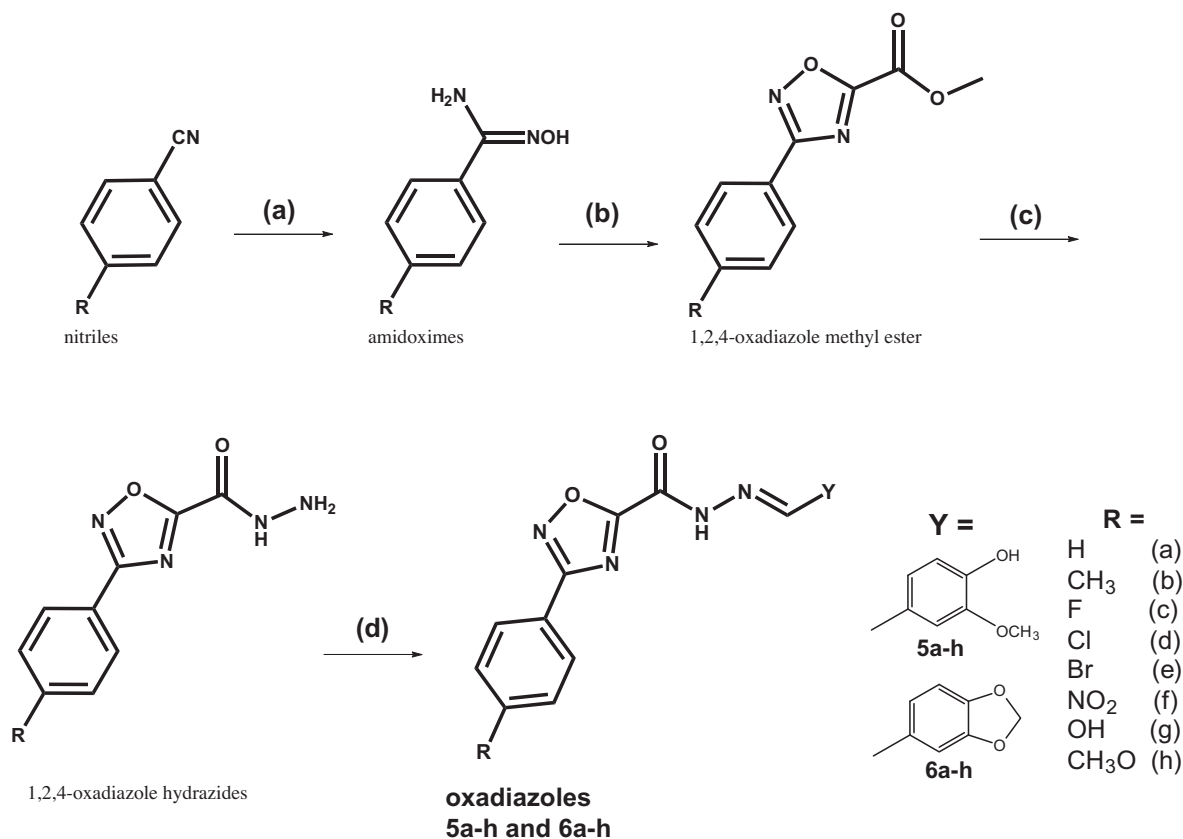
The synthesis of compounds **5a-h** and **6a-h** is depicted in Scheme 1 and is based on a method previously described by our

group.²⁵ This starts with 4-substituted aryl amidoximes, which are freshly prepared from commercially available nitriles; then they react with methyloxalyl chloride yielding the 1,2,4-oxadiazolic compounds in good yields. Further conversion of 1,2,4-oxadiazole methylesters into 1,2,4-oxadiazole hydrazides is achieved with quantitative yields by reacting them with hydrazine hydrate at 0 °C during 2 h.

These hydrazides, which are key intermediates in our research to investigate the pharmacological properties of 1,2,4-oxadiazoles,²⁶ are of easy synthesis and produces the final compounds, *N*-acylhydrazones **5a-h** and **6a-h**. To establish a SAR between our previously studied oxadiazoles (compounds **4a-h**) and oxadiazoles **5a-h** and **6a-h** described here, we used the same substituents in both cases (R = H, CH₃, F, Cl, Br, OCH₃, OH, NO₂). The σ_p -Hammett values for these substituents range from –0.37 for OH to 0.78 for NO₂, and therefore the electronic contribution of the *para*-substituent on the phenyl group varies significantly and allows us to investigate the importance of each substituent. The physical and spectroscopic data for the compounds **5a-h** are described here (experimental materials), while the spectral characterization for **6a-h** has been previously described.²⁶

N-Acylhydrazones can yield a mixture of *Z*- and *E*-isomers,²⁴ but the ¹H NMR analysis revealed that the *E*-isomers predominated (>98%). The mild conditions we used for preparing *N*-acylhydrazones **5a-h** and **6a-h** (short reaction time and room temperature) explain the predominance of the *E*-isomer in the crude products. The X-ray analysis of **6f** crystal obtained by crystallization from a dimethylformamide solution exclusively produced the *E*-diastereomer (Fig. 2), confirming the ¹H NMR data.

Quantum chemistry calculations (ab initio) suggested a planar and *E*-geometry for compounds **6a-h** and showed that two stable conformers of this geometry are possible, differing only by 2.74 kcal/mol.²⁶ The conformer of lowest energy is synperiplanar,



Scheme 1. Reagents and conditions: (a) $\text{NH}_2\text{OH}\cdot\text{HCl}$, Na_2CO_3 , $\text{H}_2\text{O}/\text{MeOH}$, reflux, 4 h; (b) $\text{ClOCCO}_2\text{CH}_3$, dry THF, reflux, 4.5 h; (c) NH_2NH_2 55%, EtOH, 0 °C, 2 h; (d) EtOH, H_2SO_4 (cat.), aromatic aldehyde, room temperature, 10 min.

with the carbonyl oxygen and the iminic hydrogen *syn* to each other. The higher stability of this conformer is because of a non-classical hydrogen bond between $\text{C}=\text{O}$ and $\text{CH}=\text{N}$, like a five-member ring. The antiperiplanar conformer has the carbonyl oxygen and the iminic hydrogen in opposite sides (*anti*), and therefore an intramolecular interaction is not possible. The conformations we predicted by quantum chemistry and the observed one by X-ray are different. The antiperiplanar conformer observed in the crystalline structure can be explained. By X-ray diffraction, the crystal structure of compound **6f** presents one molecule of DMF in the asymmetric unit. The position of the DMF molecule allows its oxygen atom to interact with two hydrogen atoms of the NAH from the imine group ($\text{CH}=\text{N}$) and the amide group ($\text{N}-\text{H}$) and it provides stability for an antiperiplanar conformer.

2.2. Pharmacology

Once the compounds had been chemically characterized, we focused on evaluating their biological activity. All compounds were evaluated against *T. cruzi*. We first assayed the cell viability of mouse splenocytes treated with oxadiazoles **5a-h** and **6a-h**. Given that the compounds showed no toxicity in this assay, having an LC_{50} higher than 100 $\mu\text{g}/\text{mL}$, they were evaluated against epimastigotes (axenic culture) and bloodstream trypomastigotes of Y strain *T. cruzi*, using benznidazole (Bdz) as a control drug. The compounds that showed IC_{50} values comparable to Bdz were further selected for in vitro and in vivo assays. The ability of these compounds to inhibit the activity of cruzain was also performed in parallel to the parasite cell assays. All compounds were initially tested at 100 μM . For active compounds, a dose–response curve was determined and the IC_{50} calculated. Table 1 summarizes the cruzain and anti-*T. cruzi* activities for oxadiazoles **5a-h** and **6a-h**.

None of the oxadiazoles **5a-h** showed anti-*T. cruzi* activity. This was an unexpected finding because compounds **5a-h** only differ from our early examined oxadiazoles (**4a-h**)²¹ by the introduction of a 3-methoxy group. But we found potent trypanosomicidal activities for oxadiazoles **6a-h**. We first noted that the halogenated oxadiazoles **6c**, **6d**, and **6e** were able to inhibit *T. cruzi*, with IC_{50} values quite similar to Bdz (Table 1). For example, oxadiazoles **6c** (fluorine) and **6d** (chlorine) have IC_{50} of 9.5 ± 2.8 and 3.5 ± 1.8 μM for Y strain trypomastigotes, quite similar to Benznidazole (IC_{50} of 11.3 ± 2.8 μM) respectively. Neither oxadiazoles **6c**, **6d**, and **6e** nor benznidazole affected the cell viability of mouse splenocytes up to 100 $\mu\text{g}/\text{mL}$, while these compounds clearly affect parasite proliferation (epimastigotes) and motility (trypomastigotes). The absence of toxicity for mouse splenocytes shows that the cell effects of oxadiazoles and Bdz are specific for *T. cruzi*.

After confirming that the oxadiazoles were able to kill *T. cruzi* parasites, our next step was to understand how these compounds affect the infection of host cells by trypomastigotes.^{27,28} We tested oxadiazoles **6c**, **6d**, and **6e** in an in vitro model of parasite infection in macrophages. Macrophages were infected with Y strain trypomastigotes and then treated with compounds at 10 $\mu\text{g}/\text{mL}$, including Bdz. Cells were analyzed by light microscopy and the percentage of infected macrophages and the number of amastigotes were determined and compared to untreated infected cells (negative control) and cells treated with benznidazole (positive control).

In untreated-infected macrophages (negative control), the percentage of infected cells is high (Figs. 3 and S1, Supplementary data). As a result, trypomastigotes complete the intracellular cycle into amastigotes, resulting in an average of almost 800 amastigotes per 100 host-cells (Fig. 3).²⁹ When 10 $\mu\text{g}/\text{mL}$ of oxadiazoles **6c** and **6d** are added, the percentage of infected macrophages is significantly reduced when compared to untreated cells. Oxadiazole **6e**,

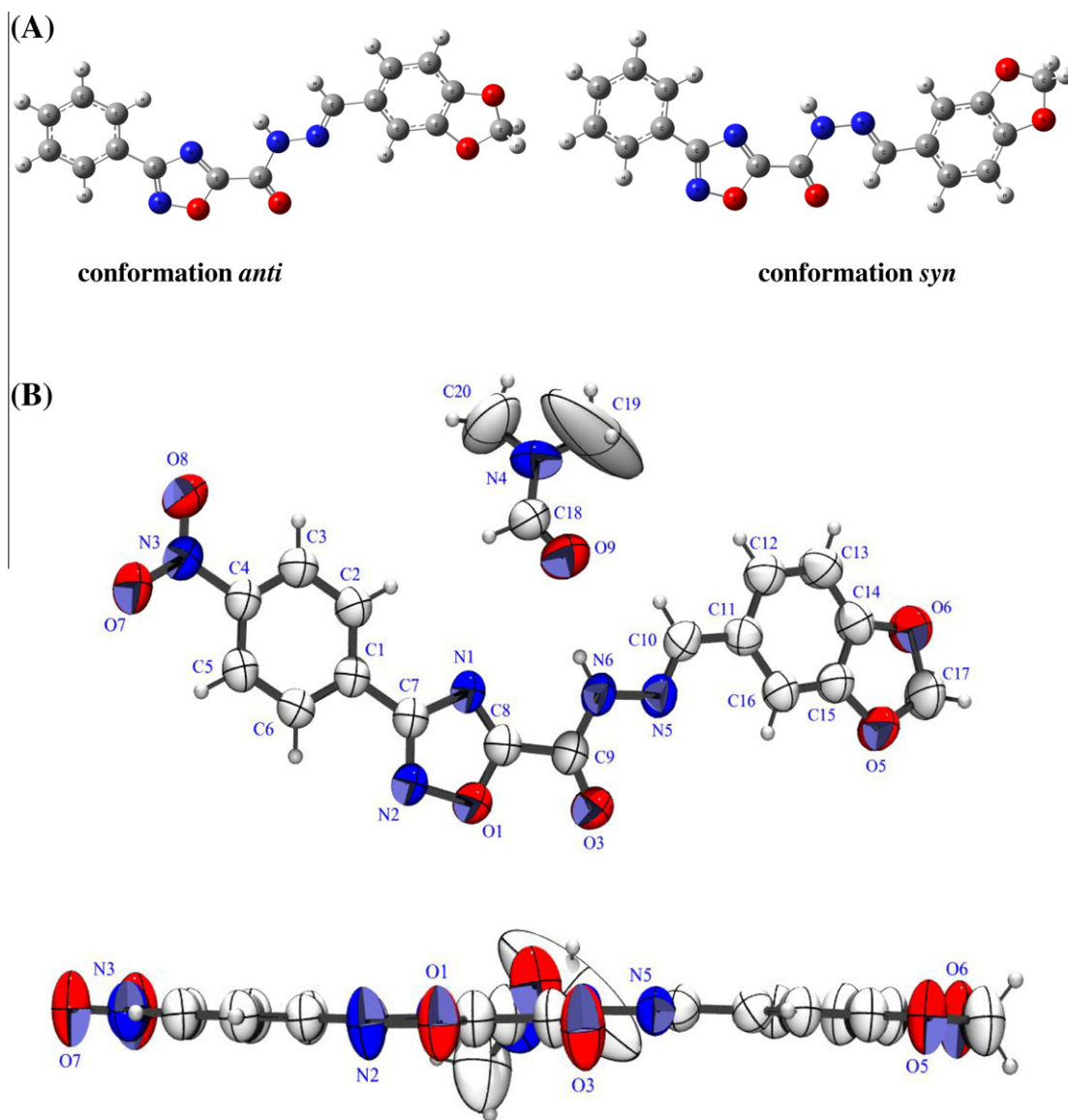


Figure 2. (A) General representation of the *syn* and *anti* conformers for oxadiazoles **6a–h**. (B) Top: structure of **6f** determined by X-ray analysis (ORTEP-3 view, displacement ellipsoids are drawn at a 50% level), highlighting the *E*-geometry and the *anti* arrangement. The bottom highlights that the molecule is entirely planar.

a bromine analog that was lethal for trypanosomes (Table 1), had no activity in these assays. When 10 $\mu\text{g}/\text{mL}$ of oxadiazoles **6c** or **6d** are added at the moment of infection, the number of infected cells is lower than untreated-infected macrophages (Fig. S2 Supplementary data). This suggests that oxadiazoles **6c** and **6d** impair trypanosome invasion into host-cells. The oxadiazoles **6c** and **6d** arrested trypanosome development and invasion of macrophages. Therefore, potency enhancement of anti-*T. cruzi* activity was achieved for oxadiazoles **6a–h** when compared to our previously studied oxadiazoles **4a–h**.²¹

We also investigated the ability of these compounds to inhibit the recombinant cysteine protease of *T. cruzi*, cruzain.¹⁸ As seen in Table 1, oxadiazoles **5d**, **5e** and **6e** showed high-affinity for cruzain (IC_{50} from 40 to 200 nM). Cruzain inhibition by these three oxadiazoles was higher when they were pre-incubated with the enzyme, consistent with a covalent-mechanism of inhibition. *N*-Acyhydrazones such as compounds **5d** and **5e** may undergo Michael-addition reactions, yielding covalent adducts with cruzain.³⁰ Other oxadiazoles of the series **5a–h** and **6a–h** did not show significant cruzain inhibition at 100 μM , so no SAR could be drawn. The cruzain inhibition observed for oxadiazoles **5d**, **5e** and **6e** was not

due to nonspecific binding. The assay was repeated in the absence and the presence of 0.1% Triton X-100.¹⁸ The level of cruzain inhibition did not vary among these conditions, suggesting that enzyme inhibition is not due to compound aggregation. Since there is no reliable correlation between cruzain inhibition and trypanosomicidal properties, the trypanosomicidal effects of oxadiazoles are only in part due to cruzain inhibition, other targets and biochemical pathways must be involved.

To further investigate the mechanism of action of oxadiazoles **6c** and **6d**, ultrastructural alterations in bloodstream trypanosomes were analyzed. Electron micrographs are shown in Figure 4. In comparison to untreated parasites, trypanosomes incubated with **6c** and **6d** had membrane protrusions in about 80% of cells. Oxadiazoles **6c** and **6d** caused mitochondria degeneration, Golgi apparatus and endoplasmic reticulum disorganization, followed by kinetoplast enlargement. When infected macrophages were treated with 3.5 μM of oxadiazole **6d**, we could observe that oxadiazole **6d** targets mitochondria, causing fragmentation as well as the formation of atypical vacuoles which contain mitochondrial components (Fig. 5). High-affinity cruzain inhibitors, such as peptide K777, are believed to induce structural alterations in Golgi

Table 1
Cruzain and anti-*T. cruzi* activities

| Compound | R | % Cruzain inhibition 100 μM^a | Y strain <i>T. cruzi</i> IC ₅₀ μM (\pm SD) | | Mouse splenocytes LC ₅₀ ^d ($\mu\text{g}/\text{mL}$) |
|-------------------------|-------------------|--|---|----------------------------|--|
| | | | Trypomastigotes ^b | Epimastigotes ^c | |
| | | | | | |
| 5a | H | 47 | ND | ND | >100 |
| 5b | CH ₃ | 14 | ND | ND | >100 |
| 5c | F | 63 | ND | ND | >100 |
| 5d | Cl | 92 (0.04) | ND | ND | >100 |
| 5e | Br | 100 (0.2) | ND | ND | >100 |
| 5f | NO ₂ | 47 | ND | ND | >100 |
| 5g | OH | 25 | ND | ND | >100 |
| 5h | CH ₃ O | 35 | ND | ND | >100 |
| | | | | | |
| 6a | H | 32 | ND | ND | >100 |
| 6b | CH ₃ | 49 | ND | ND | >100 |
| 6c | F | 34 | 9.5 (\pm 2.8) | 12.2 (\pm 7.6) | >100 |
| 6d | Cl | 42 | 3.5 (\pm 1.8) | 7.5 (\pm 4.8) | >100 |
| 6e | Br | 95 (0.03) | 13.4 (\pm 1.8) | 14.0 (\pm 5.4) | >100 |
| 6f | NO ₂ | NT | ND | ND | >100 |
| 6g | OH | 17 | ND | ND | >100 |
| 6h | CH ₃ O | 44 | ND | ND | >100 |
| Bdz ^e | — | — | 11.3 (\pm 1.8) | 7.5 (\pm 2.1) | — |
| GV ^e | — | — | — | — | 0.11 |

^a Cruzain inhibition after a 10 min pre-incubation with the inhibitor. The results represent the average of duplicates. Values in parenthesis represent IC₅₀ values in μM , which were determined based on at least 9 compound concentrations in duplicate.

^b Determined after 24 h of incubation of trypomastigotes with the compounds. Values were calculated from five concentrations using data obtained from at least two independent experiments (SD given in parenthesis).

^c Determined after 5 days of incubation of epimastigotes with the compounds. IC₅₀ was calculated from five concentrations using data obtained from at least two independent experiments (SD given in parenthesis).

^d Toxicity for splenocytes of BALB/c mouse after 24 h of incubation in the presence of the compounds.

^e Bdz = Benznidazole; GV = Gentian Violet. Nd., not determined, due to the lack of activity in the tested concentration. SD = standard deviation.

apparatus, endoplasmic reticulum, and to alter protein trafficking into lysosomes/reservosomes.³¹ Alterations of mitochondria and kinetoplast are not observed for well-known cruzain inhibitors.^{31,32} These information differed from those observed here for oxadiazoles **6c** and **6d**. What we observed is that oxadiazoles substantially alter the mitochondrial morphology, therefore proteins involved in parasite metabolism and bioenergetics might be the molecular targets for oxadiazoles. Instead of attempting to identify these target proteins, we decided to evaluate whether these compounds reduce blood parasitemia in *T. cruzi*-infected mice.

To determine the maximum tolerated dose (MTD), single oral treatment of oxadiazole **6d** to uninfected BALB/c mice ($n = 3/\text{group}$) at doses of 25, 50, and 100 mg/kg was performed. Mice treated with **6d** appeared normal and no mortality was observed. We also measured serum biochemical components in uninfected mice treated with **6d** (Table S1). In comparison to untreated and uninfected mice, treatment with **6d** did not systematically change serum components, suggesting the toxicity of these oxadiazoles is not a major concern. Based on this, oxadiazoles **6c** and **6d** were administered at dose of 50 mg/kg to infected mice.

BALB/c mice were infected with Y strain trypomastigotes³³ and treated or not with **6c**, **6d**, and Bdz. In untreated, infected mice, blood parasitemia was observed after day 8 of parasite inoculation and peaked on day 10 (Fig. 6). Benznidazole (Bdz) gi-

ven orally at 100 mg/kg once a day for 5 days (starting from day 5 after infection) almost eradicated blood parasitemia. Compound **6d** substantially reduced blood parasitemia ($p < 0.001$) compared to untreated infected mice. Compound **6c** did not reduce parasitemia as much as compound **6d**, as expected based on its lower potency. Compound **6e** was not tested due to low solubility.

N-Acyhydrazones are known for their in vitro trypanosomicidal and cruzain inhibition effects.^{34–37} However, very few *N*-acyhydrazones that are effective in reducing in vivo infection have been identified.³⁸ One method for increasing the efficacy of anti-*T. cruzi* *N*-acyhydrazones is through the combination with oxadiazole chemistry.^{19–21} From our past studies, we discovered that *N*-acyhydrazones derived from 1,2,4-oxadiazole chemistry were less potent trypanosomicidal agents than benznidazole, but at least they were more selective for parasite than to mammalian cells.²¹ Here, our main aim was to improve the cidal potency by molecular modification. We knew from past SAR model that the *N*-acyhydrazone motif is more suitable and tolerates molecular modification. In view of this, we planned compounds **5a–h** and **6a–h**. This structural design was successful and led us to identify the anti-*T. cruzi* oxadiazole denoted **6d**.

We believe that compound **6d** merits further chemical optimization because: (a) it has a selectivity window of at least 50 (host cell

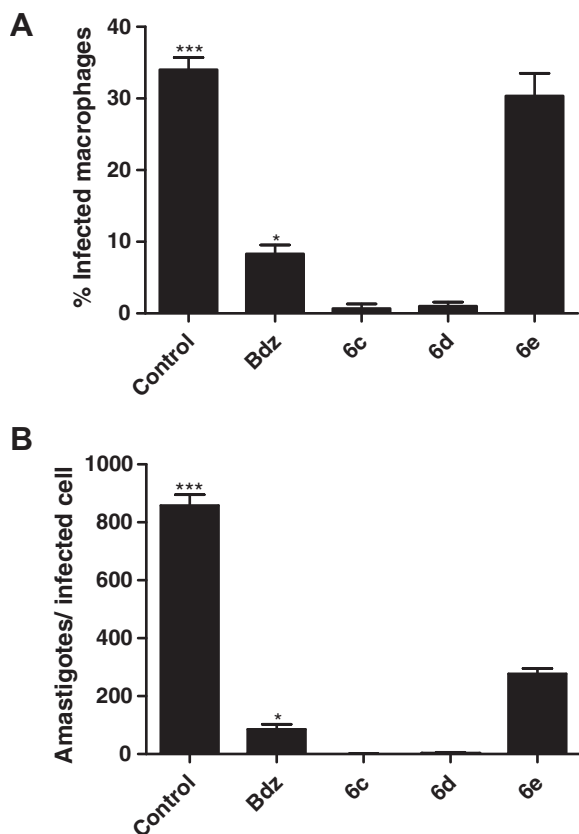


Figure 3. Oxadiazoles impair *T. cruzi* trypomastigote development in macrophages. The percentage of infected macrophages (A) and the mean number of amastigotes/infected cell (B) are higher in untreated infected controls than in cultures treated with 10 $\mu\text{g}/\text{mL}$ of test-inhibitors **6c** or **6d**. Bdz is benznidazole. Experiment done in triplicate. Standard deviations are shown as error bars. ***, $p < 0.001$; *, $p < 0.05$.

toxicity $\text{LC}_{50}/T. cruzi \text{IC}_{50}$); (b) it is efficient and well-tolerated in oral treatment; (c) at a dose of 50 mg/kg (140 $\mu\text{mol}/\text{kg}$) parasitemia was reduced in vivo; (d) **6d** is a low-molecular weight, achiral, and nonpeptidic compound. These functional properties and chemical features are desirable for a Chagas disease drug candidate.³⁹

3. Conclusions

From our past studies, oxadiazoles were less potent cidal than benznidazole, but they were more selective for parasite versus mammalian cells. Here, our effort was to improve their cidal potency by molecular modification of substituents. To this end, trypanosomicidal properties as well cruzain inhibition of 3-aryl-1,2,4-oxadiazole-5-carbohydrazides containing a 4-hydroxy-3-methoxyphenyl **5a–h** or 1,3-benzodioxole **6a–h** were determined. Oxadiazole **6d**, which features a 1,3-benzodioxole group near to the *N*-acylhydrazone was identified as the most potent and selective trypanosomicidal compound among them, and endowed with efficacy in reducing blood parasitemia in a mouse model of acute infection. The efficacy observed for oxadiazole **6d** in in vitro and in vivo models of infection argues favorably for oxadiazoles as antiparasitic agents and therefore the synthetic redesign of variant forms of oxadiazole **6d** is worthy.

4. Experimental section

4.1. Chemistry

Melting points were determined on a Gallenkamp capillary apparatus and are uncorrected. Infrared spectra were determined

using KBr discs on a Perkin–Elmer Paragon 500 FT-IR spectrometer. ^1H NMR spectra were determined on a Bruker DPX-200 spectrometer, with chemical shifts δ reported in ppm unities relative to the internal standard TMS, using $\text{DMSO-}d_6$ as solvent. Mass spectral were determined by using a Finnigan mass spectrometers model MAT 8200 for low resolution mass spectrometry (MS) and the MAT 95 for high resolution mass spectrometry (HRMS). Values for HRMS lie within the permitted limit intervals with resolution of 10,000. The reactions were monitored by thin layer chromatography (TLC), performed on plates prepared with a 0.2 mm thick silica gel 60 (PF-254 with gypsum, Merck). The developed chromatograms were visualized under ultraviolet light at 254–265 nm. For column chromatography, silica gel 60 (230–400 mesh, Merck) was used. All common laboratory chemicals were purchased from commercial sources and used without previous purification. Crystallographic data for compound **6f** can be obtained free of charge at the Cambridge Crystallographic Data Centre (CCDC, deposit number 870707, www.ccdc.cam.ac.uk/data_request/cif).

4.1.1. General procedure for preparation of compounds **5a–h**

To a stirred suspension of 0.01 mol of appropriate hydrazide in 5 mL of ethanol, 3–4 drops of concentrated sulfuric acid were added, changing the mixture to a clear solution. Then, vanillin (0.01 mol) previously dissolved in 5 mL of ethanol was added to the mixture at room temperature. After few seconds, a colored solid precipitated and the mixture was stirred for 10 min before the addition of 10 mL of water. After vacuum filtration, the solid was washed with cold water/ethanol 1:1 and then with cold water. Recrystallization from dioxane/water mixture afforded the crystalline solids. Yields, melting points, spectroscopic and spectrometric data are listed below for each compound.

4.1.1.1. 3-Phenyl-*N'*-[(4-hydroxy-3-methoxyphenyl)methylene]-1,2,4-oxadiazole-5-carbohydrazide (5a**).** Yield: 91%; Mp 216 °C (from dioxane/ H_2O); IR (KBr, cm^{-1}): $\nu = 3494$ (br O–H), 3448 (N–H, acyl hydrazone), 3190 (C–H, imine), 1674 (C=O), 1594 (C=N, imine), 1516 (C=N, heterocyclic). ^1H NMR (200 MHz, $\text{DMSO-}d_6$) δ : 12.6 (s, 1H, CONH), 9.71 (s, 1H, OH), 8.48 (s, 1H, N=CH), 8.09–8.06 (m, 2H, ortho to oxadiazole ArH), 7.63–7.59 (m, 3H, meta/para to oxadiazole ArH), 7.31 (s, 1H, 2 to hydrazone ArH), 7.11 (d, 1H, $^3J = 8.3$ Hz, 6 to hydrazone ArH), 6.84 (d, 1H, $^3J = 7.8$ Hz, 5 to hydrazone ArH), 3.82 (s, 3H, OCH_3). MS (m/z): 338 (M^+ , 100), 192 (M-phenyloxadiazole, 14), 164 (192-CO, 6), 149 (192-HNCO, 43), 136 (164- N_2 , 70). HRMS for $\text{C}_{17}\text{H}_{14}\text{N}_4\text{O}_4$ calcd (found): 338.10151 (338.10238).

4.1.1.2. 3-(4-Methylphenyl)-*N'*-[(4-hydroxy-3-methoxyphenyl)methylene]-1,2,4-oxadiazole-5-carbohydrazide (5b**).** Yield: 92%; Mp 213 °C (from dioxane/ H_2O); IR (KBr, cm^{-1}): $\nu = 3479$ (br O–H; N–H, acyl hydrazone), 3181 (C–H, imine), 1702 (C=O), 1607 (C=N, imine), 1515 (C=N, heterocyclic). ^1H NMR (200 MHz, $\text{DMSO-}d_6$) δ : 12.6 (s, 1H, CONH), 9.70 (s, 1H, OH), 8.47 (s, 1H, N=CH), 7.97 (d, 2H, $^3J = 8.1$ Hz, ortho to oxadiazole ArH), 7.41 (d, 2H, $^3J = 8.1$ Hz, meta to oxadiazole ArH), 7.31 (d, 1H, $^4J = 1.7$ Hz, 2 to hydrazone ArH), 7.10 (dd, 1H, $^4J = 1.7$ Hz, $^3J = 8.4$ Hz, 6 to hydrazone ArH), 6.84 (d, 1H, $^3J = 8.4$ Hz, 5 to hydrazone ArH), 3.82 (s, 3H, OCH_3), 2.38 (s, 3H, CH_3). MS (m/z): 352 (M^+ , 100), 192 (M-phenyloxadiazole, 14), 164 (192-CO, 3), 149 (192-HNCO, 60), 136 (164- N_2 , 78). HRMS for $\text{C}_{18}\text{H}_{16}\text{N}_4\text{O}_4$ calcd (found): 352.11716 (352.11712).

4.1.1.3. 3-(4-Fluorophenyl)-*N'*-[(4-hydroxy-3-methoxyphenyl)methylene]-1,2,4-oxadiazole-5-carbohydrazide (5c**).** Yield: 90%; Mp 216 °C (from dioxane/ H_2O); IR (KBr, cm^{-1}): $\nu = 3486$ (br O–H), 3446 (N–H, acyl hydrazone), 3197 (C–H, imine), 1677

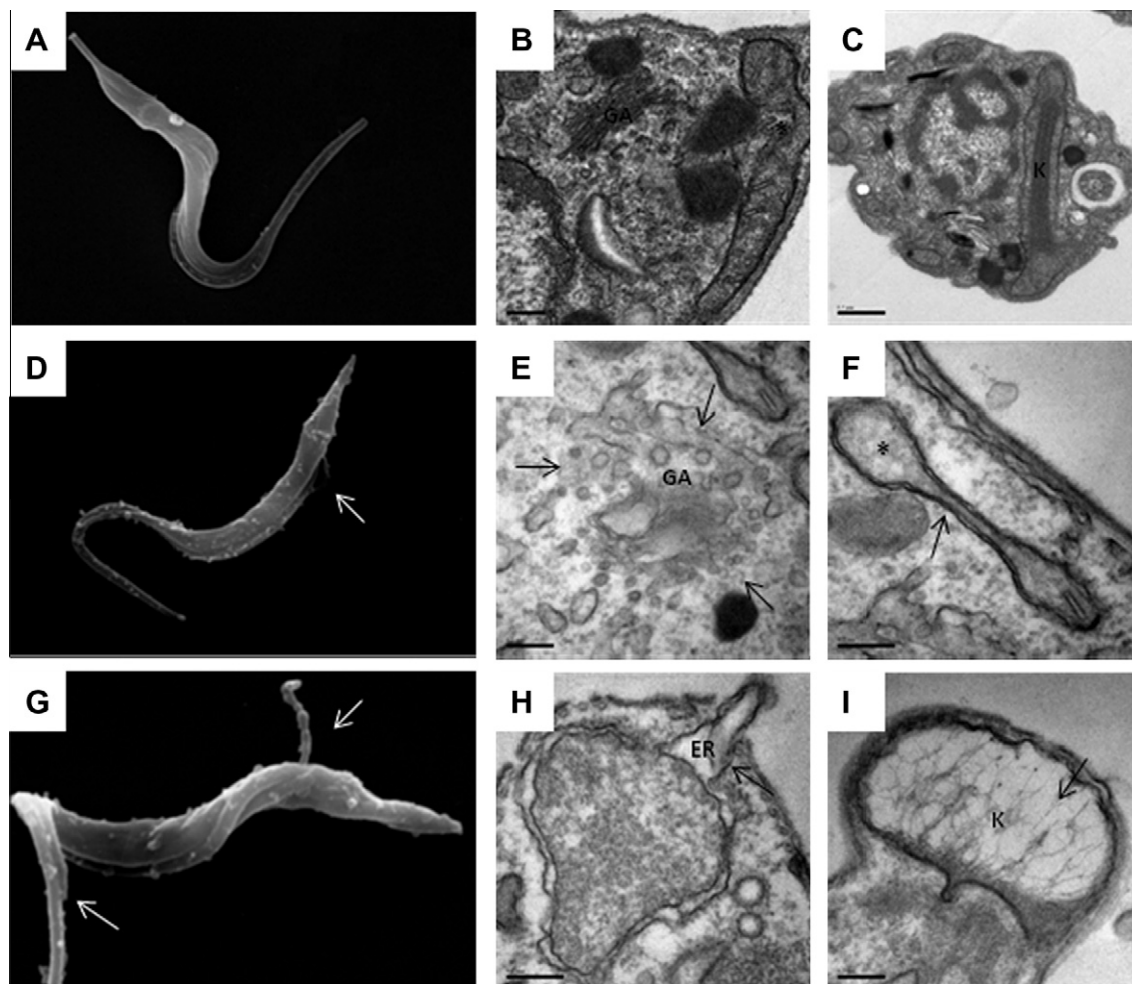


Figure 4. Oxadiazoles induce ultrastructural changes in bloodstream trypomastigotes. Using SEM, we observed plasma membrane protrusions (arrows) in cells treated with compounds **6c** (30 μ M; D) or **6d** (10 μ M; G); untreated cells (A). Using TEM, untreated trypomastigotes highlighting Golgi apparatus and mitochondria (B) and kinetoplast (C). In cells treated with **6c** (9.5 μ M, E, F) or **6d** (3.5 μ M, H, I), we observed alterations in Golgi apparatus (E), mitochondria (F), membranes of endoplasmic reticulum (H), and kinetoplast (I). GA = Golgi apparatus; * = Mitochondria; ER = endoplasmic reticulum; K = kinetoplast.

(C=O), 1592 (C=N, imine), 1516 (C=N, heterocyclic). ^1H NMR (200 MHz, DMSO- d_6) δ : 12.6 (s, 1H, CONH), 9.70 (s, 1H, OH), 8.47 (s, 1H, N=CH), 8.13 (dd, 2H, $^4J_{F-H} = 5.2$ Hz, $^3J = 8.8$ Hz, ortho to oxadiazole ArH), 7.46 (t, 2H, $J = 8.8$ Hz, meta to oxadiazole ArH), 7.3 (d, 1H, $^4J = 1.3$ Hz, 2 to hydrazone ArH), 7.11 (dd, 1H, $^4J = 1.3$ Hz, $^3J = 8.2$ Hz, 6 to hydrazone ArH), 6.84 (d, 1H, $^3J = 7.9$ Hz, 5 to hydrazone ArH), 3.82 (s, 3H, OCH₃). MS (m/z , %): 356 (M^+ , 100), 192 (M-phenyloxadiazole, 14), 164 (192-CO, 6), 149 (192-HNCO, 68), 136 (164-N₂, 72). HRMS Calcd for C₁₇H₁₃N₄O₄F calcd (found): 356.09208 (356.09178).

4.1.1.4. 3-(4-Chlorophenyl)-N'-[(4-hydroxy-3-methoxyphenyl)methylene]-1,2,4-oxadiazole-5-carbohydrazide (5d). Yield: 88%; Mp 219 °C (from dioxane/H₂O); IR (KBr, cm⁻¹): $\nu = 3501$ (br O-H), 3446 (N-H, acyl hydrazone), 3223 (C-H, imine), 1678 (C=O), 1591 (C=N, imine), 1517 (C=N, heterocyclic). ^1H NMR (200 MHz, DMSO- d_6) δ : 12.6 (s, 1H, CONH), 9.71 (s, 1H, OH), 8.47 (s, 1H, N=CH), 8.09 (d, 2H, $^3J = 8.5$ Hz, ortho to oxadiazole ArH), 7.69 (d, 2H, $J = 8.1$ Hz, meta to oxadiazole ArH), 7.30 (d, 1H, $^4J = 1.3$ Hz, 2 to hydrazone ArH), 7.11 (dd, 1H, $^4J = 1.3$ Hz, $^3J = 9.8$ Hz, 6 to hydrazone ArH), 6.84 (d, 1H, $^3J = 8.1$ Hz, 5 to hydrazone ArH), 3.82 (s, 3H, OCH₃). MS (m/z , %): 372/375 (M^+ , 100/34), 192 (M-phenyloxadiazole, 21), 164 (192-CO, 7), 149 (192-HNCO, 97), 136 (164-N₂, 98). HRMS for C₁₇H₁₃N₄O₄Cl calcd (found): 372.06253 (372.06334).

4.1.1.5. 3-(4-Bromophenyl)-N'-[(4-hydroxy-3-methoxyphenyl)methylene]-1,2,4-oxadiazole-5-carbohydrazide (5e). Yield: 88%; Mp 212 °C (from dioxane/H₂O); IR (KBr, cm⁻¹): $\nu = 3329$ (br O-H), 3217 (N-H, acyl hydrazone), 3190 (C-H, imine), 1674 (C=O), 1583 (C=N, imine), 1516 (C=N, heterocyclic). ^1H NMR (200 MHz, DMSO- d_6) δ : 12.7 (s, 1H, CONH), 9.70 (s, 1H, OH), 8.47 (s, 1H, N=CH), 8.02 (d, 2H, $^3J = 8.5$ Hz, ortho to oxadiazole ArH), 7.83 (d, 2H, $J = 8.5$ Hz, meta to oxadiazole ArH), 7.30 (d, 1H, $^4J = 1.3$ Hz, 2 to hydrazone ArH), 7.11 (dd, 1H, $^4J = 1.3$ Hz, $^3J = 8.2$ Hz, 6 to hydrazone ArH), 6.84 (d, 1H, $^3J = 7.8$ Hz, 5 to hydrazone ArH), 3.82 (s, 3H, OCH₃). MS (m/z , %): 416/418 (M^+ , 59/59), 192 (M-phenyloxadiazole, 21), 164 (192-CO, 7), 149 (192-HNCO, 100), 136 (164-N₂, 97). HRMS for C₁₇H₁₃N₄O₄Br calcd (found): 416.01202 (416.01187).

4.1.1.6. 3-(4-Nitrophenyl)-N'-[(4-hydroxy-3-methoxyphenyl)methylene]-1,2,4-oxadiazole-5-carbohydrazide (5f). Yield: 91%; Mp 383 °C (from dioxane/H₂O); IR (KBr, cm⁻¹): $\nu = 3490$ (br O-H), 3280 (N-H, acyl hydrazone), 1697 (C=O), 1596 (C=N, imine), 1513 (C=N, heterocyclic). ^1H NMR (200 MHz, DMSO- d_6) δ : 12.8 (s, 1H, CONH), 9.70 (s, 1H, OH), 8.48 (s, 1H, N=CH), 8.46 (d, 2H, $^3J = 9.3$ Hz, meta to oxadiazole ArH), 8.34 (d, 2H, $^3J = 8.8$ Hz, ortho to oxadiazole ArH), 7.31 (d, 1H, $^4J = 1.3$ Hz, 2 to hydrazone ArH), 7.12 (dd, 1H, $^4J = 1.3$ Hz, $^3J = 8.3$ Hz, 6 to hydrazone ArH), 6.85 (d, 1H, $^3J = 8.3$ Hz, 5 to hydrazone ArH), 3.82 (s,

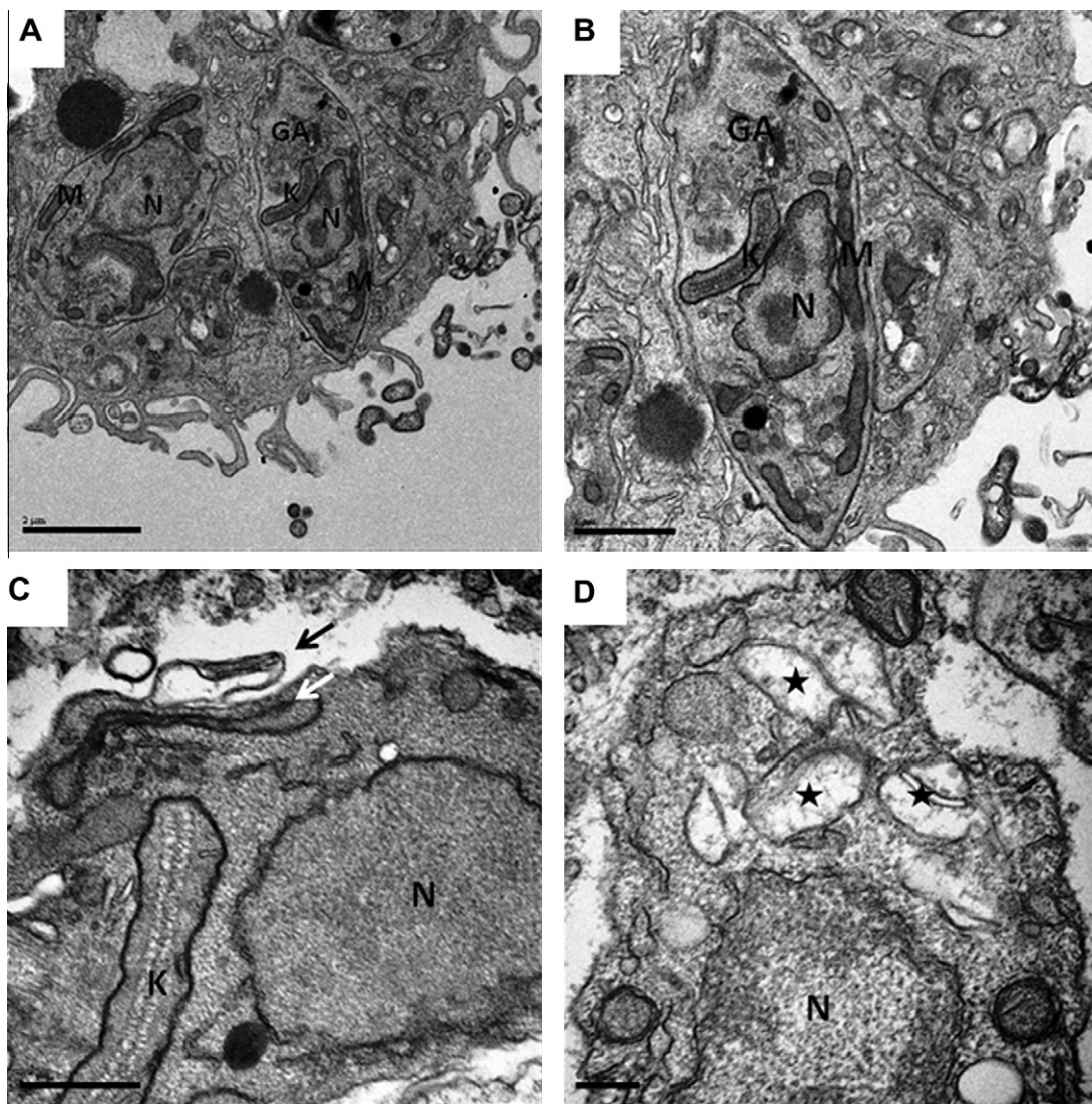


Figure 5. Oxadiazole **6d** induces structural changes in intracellular amastigotes. (A and B) TEM of untreated cells highlighting nucleus (N) and Golgi apparatus (GA). (C and D) in cells treated with 3.25 μM of **6d** we observed alterations in membrane (black arrow), degradation of mitochondria (white arrow) as well atypical mitochondrial vacuoles (black stars). Scale of 2.0 (A), 1.0 (B), 0.5 (C), and 0.2 μm (D).

3H, OCH₃). MS (*m/z*,%): 383 (M⁺, 100), 192 (M-phenyloxadiazole, 18), 164 (192-CO, 6), 149 (192-HNCO, 73), 136 (164-N₂, 62). HRMS for C₁₇H₁₃N₅O₆ calcd (found): 383.08658 (383.08753).

4.1.1.7. 3-(4-Hydroxyphenyl)-N-[(4-hydroxy-3-methoxyphenyl)methylene]-1,2,4-oxadiazole-5-carbohydrazide (5g).

Yield: 99%; Mp 264 °C (from dioxane/H₂O); IR (KBr, cm⁻¹): ν = 3518, 3499 (O-H), 3293 (N-H, acyl hydrazone), 1693 (C=O), 1596 (C=N, imine), 1512 (C=N, heterocyclic). ¹H NMR (200 MHz, DMSO-*d*₆) δ : 12.6 (s, 1H, CONH), 10.2 (s, 1H, para to oxadiazole OH), 9.69 (s, 1H, OH), 8.46 (s, 1H, N=CH), 7.91 (d, 2H, ³J = 8.8 Hz, ortho to oxadiazole ArH), 7.30 (d, 1H, ⁴J = 1.3 Hz, 2 to hydrazone ArH), 7.11 (dd, 1H, ⁴J = 1.5 Hz, ³J = 8.2 Hz, 6 to hydrazone ArH), 6.94 (d, 2H, ³J = 8.8 Hz, meta to oxadiazole ArH), 6.84 (d, 1H, ³J = 8.2 Hz, 5 to hydrazone ArH), 3.82 (s, 3H, OCH₃). MS (*m/z*,%): 354 (M⁺, 100), 192 (M-phenyloxadiazole, 8), 164 (192-CO, 3), 149 (192-HNCO, 32), 136 (164-N₂, 42). HRMS for C₁₇H₁₄N₄O₅ calcd (found): 354.09642 (354.09733).

4.1.1.8. 3-(4-Methoxyphenyl)-N-[(4-hydroxy-3-methoxyphenyl)methylene]-1,2,4-oxadiazole-5-carbohydrazide (5h).

Yield: 97%; Mp 221 °C (from dioxane/H₂O); IR (KBr, cm⁻¹): ν = 3500–

3000 (br O-H), 3415 (N-H, acyl hydrazone), 1677 (C=O), 1597 (C=N, imine), 1512 (C=N, heterocyclic). ¹H NMR (200 MHz, DMSO-*d*₆) δ : 12.6 (s, 1H, CONH), 9.70 (s, 1H, OH), 8.47 (s, 1H, N=CH), 8.02 (d, 2H, ³J = 8.9 Hz, ortho to oxadiazole ArH), 7.31 (d, 1H, ⁴J = 1.3 Hz, 2 to hydrazone ArH), 7.15 (d, 2H, ³J = 8.6 Hz, meta to oxadiazole ArH), 7.11 (dd, 1H, ⁴J = 1.3 Hz, ³J = 8.3 Hz, 6 to hydrazone ArH), 6.84 (d, 1H, ³J = 8.3 Hz, 5 to hydrazone ArH), 3.84 (s, 3H, para to oxadiazole OCH₃), 3.82 (s, 3H, OCH₃). MS (*m/z*,%): 368 (M⁺, 100), 192 (M-phenyloxadiazole, 10), 164 (192-CO, 4), 149 (192-HNCO, 35), 136 (164-N₂, 42). HRMS for C₁₈H₁₆N₄O₅ calcd (found): 368.11207 (368.11232).

4.2. Animals

Female BALB/c mice (6–8 weeks old) were supplied by the animal breeding facility at Centro de Pesquisas Gonçalo Moniz (Fundação Oswaldo Cruz, Bahia, Brazil) and maintained in sterilized cages under a controlled environment, receiving a balanced diet for rodents and water ad libitum. All experiments were carried out in accordance with the recommendations of Ethical Issues Guidelines, and were approved by the local Animal Ethics Committee.

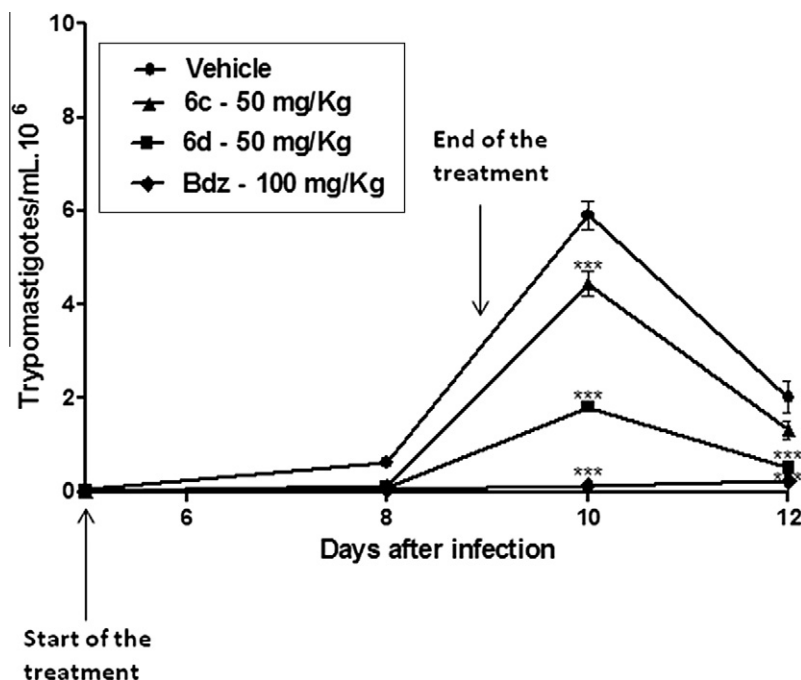


Figure 6. Oxadiazole **6d** substantially reduces parasitemia in mice. Female BALB/c mice were infected with 10^4 Y strain trypomastigotes. Five days after infection, mice were treated orally with compounds **6c** and **6d** in one daily dose of 50 mg/kg or Benznidazole (Bdz, at 100 mg/kg), during five consecutive days. Parasitemia was monitored by counting the number of trypomastigotes in fresh blood samples. Values represent the mean \pm SEM of six mice per group. Two independent experiments, data are from one experiment. ***, $p < 0.001$ compared to untreated-infected group (vehicle).

4.3. Parasites

Epimastigotes of *T. cruzi* (Y strain) were maintained at 26 °C in LIT medium (Liver Infusion Tryptose) supplemented with 10% fetal bovine serum (FBS) (Cultilab, Campinas, SP, Brazil), 1% hemin (Sigma Co, St. Louis, MO, USA), 1% R9 medium (Sigma Co), and 50 μ g/mL gentamycin (Novafarma, Anápolis, GO, Brazil). Bloodstream trypomastigotes forms of *T. cruzi* were obtained from supernatants of LLC-MK₂ cells previously infected and maintained in RPMI-1640 medium (Sigma Co.) supplemented with 10% FBS, and 50 μ g/mL gentamycin at 37 °C and 5% CO₂.

4.4. Cruzain inhibition

Cruzain activity was measured by monitoring the cleavage of the fluorogenic substrate Z-Phe-Arg-aminomethylcoumarin (Z-FR-AMC), as previously described.¹⁸ All assays were performed in 96-well plate format, in a final volume of 200 μ L, in sodium acetate 0.1 M (pH 5.5), in the presence of 5 mM dithiothreitol (DTT) and 0.01% Triton X-100, except for evaluation of detergent-sensitivity, when inhibition was also evaluated in 0% and 0.1% Triton for comparison. The enzyme was present at the final concentration of 0.4 nM and the substrate at 2.5 μ M ($K_m = 2 \mu$ M). All assays were performed in duplicate and followed for 5 min, and cruzain activity was calculated based on initial rates of substrate cleavage compared to a DMSO control. All compounds were dissolved in DMSO. The initial screen was performed at 100 μ M of each compound. Compounds were first evaluated for time-dependence by comparing percentages of enzyme inhibition by a compound with or without pre-incubation with enzyme for 10 min. During the pre-incubation step, cruzain and compound concentrations were 10-fold higher than in the final assay. Since compounds were observed to be time-dependent, consistently with a covalent mode of inhibition, all subsequent assays were performed with a 10 min pre-incubation. Compounds which inhibited over 50% of cruzain activity at 100 μ M had their IC₅₀ determined and were further evalu-

ated for detergent-sensitivity. Dose–response curves were determined based on at least nine compounds concentrations, varying from 100 μ M to 0.1 nM in fourfold dilutions. Data was analyzed with Prism 4 (GraphPad) employing non-linear regression.

4.5. Cytotoxicity to mouse splenocytes

Splenocytes obtained from BALB/c mice were placed into 96-well plates at a cell density of 5×10^6 cells/well in RPMI-1640 medium supplemented with 10% of FBS and 50 μ g mL⁻¹ of gentamycin. Each test inhibitor was used in five concentrations (1.23, 3.70, 11.11, 33.33, and 100 μ g mL⁻¹) in triplicate. To each well, an aliquot of test inhibitor suspended in DMSO was added. Controls included wells only containing either solvent (untreated cells) or gentian violet (positive control). The plate was incubated for 24 h at 37 °C and 5% CO₂. After incubation, 1.0 μ Ci of ³H-thymidine (Perkin Elmer, Waltham, USA) was added to each well, and the plate was returned to the incubator. The plate was then transferred to a beta-radiation counter (Multilabel Reader, Finland), and the percent of ³H-thymidine was determined. Cell viability was measured as the percent of ³H-thymidine incorporation for treated-cells in comparison to untreated cells. LD₅₀ values were calculated using data-points gathered from two independent experiments.

4.6. Antiproliferative activity for epimastigotes

Epimastigotes were counted in a hemocytometer and then dispensed into 96-well plates at a cell density of 10^6 cells/well. Test inhibitors, dissolved in DMSO, were diluted into five different concentrations (1.23, 3.70, 11.11, 33.33, and 100 μ g/mL) and added to the respective wells in triplicate. The plate was incubated for 5 days at 26 °C, and aliquots of each well were collected and the number of viable parasites were counted in a Neubauer chamber, and compared to untreated parasite culture. IC₅₀ calculation was carried out using non-linear regression on Prism 4.0 GraphPad

software. This experiment was done in triplicate, and benznidazole (LAFEPE, Pernambuco, Brazil) was used as the reference inhibitor.

4.7. Cytotoxicity for trypomastigotes

Trypomastigotes collected from the supernatants of LLC-MK₂ cells were dispensed into 96-well plates at a cell density of 4×10^5 cells/well. Test inhibitors, dissolved in DMSO, were diluted into five different concentrations and added into their respective wells, and the plate was incubated for 24 h at 37 °C and 5% of CO₂. Aliquots of each well were collected and the number of viable parasites, based on parasite motility, was assessed in a Neubauer chamber. The percentage of inhibition was calculated in relation to untreated cultures. IC₅₀ calculation was also carried out using a non-linear regression with Prism 4.0 GraphPad software. This experiment was repeated once, and benznidazole was used as the positive control.

4.8. Trypomastigote development

Peritoneal exudate macrophages were seeded at a cell density of 2×10^5 cells/well in a 24 well-plate with rounded coverslips on the bottom in RPMI supplemented with 10% FBS and incubated for 24 h. Cells were then infected with trypomastigotes at a ratio of 10 parasites per macrophage for 2 h. Free trypomastigotes were removed by successive washes using saline solution. Each test inhibitor was dissolved in DMSO at 10 µg/mL and incubated for 6 h. The medium was replaced by a fresh medium and the plate was incubated for 4 days. Cells were fixed in methanol and the percentage of infected macrophages and the mean number of amastigotes/infected macrophages was determined by manual counting after Giemsa staining in an optical microscope (Olympus, Tokyo, Japan). The percentage of infected macrophages and the number of amastigotes per macrophage was determined by counting 100 cells per slide.

4.9. Trypomastigote invasion

Peritoneal macrophages (10^5 cells) were plated onto 13-mm glass coverslips in 24-well plate and kept for 24 h. The plate was washed with saline solution and then trypomastigotes were added at a cell density of 1.25×10^7 along with the addition of test inhibitor (stock solution at 10 µg/mL). The plate was incubated for 2 h at 37 °C and 5% CO₂, followed by five washes with saline solution to remove extracellular trypomastigotes. Plates were maintained in RPMI medium supplemented with 10% FBS at 37 °C for 2 h. Infected cells were examined for the presence of amastigotes by optical microscopy using a standard Giemsa staining.

4.10. Ultrastructural studies

Trypomastigotes at a cell density of 3×10^7 were treated with test inhibitors **6c** (9.5 µM) and **6d** (3.5 µM) for 24 h. Parasites were then fixed with 2% formaldehyde and 2.5% glutaraldehyde (Electron Microscopy Sciences, PA, USA) in sodium cacodylate buffer (0.1 M, pH 7.2) for 1 h at room temperature. After fixation, parasites were washed three times with sodium cacodylate buffer (0.1 M, pH 7.2), and post-fixed with a 1.0% solution of osmium tetroxide (Sigma Chemical Co., MO, USA) for 1 h. Cells were subsequently dehydrated in increasing concentrations of acetone (30%, 50%, 70%, 90% and 100%) for 10 min at each step and embedded in resin Polybed (PolyScience family, Warrington, PA, USA). Ultrathin sections were prepared on an ultramicrotome Leica UC7 and sections were collected on copper grids of 300 meshes, contrasted with uranyl acetate and lead citrate and ob-

served under a JEOL TEM-1230 transmission electron microscope. For scanning electron microscopy, trypomastigotes treated with **6c** (30 µM) or **6d** (10 µM) and fixed in the same conditions were washed in 0.1 M cacodylate buffer, and allowed to adhere in coverslips pre-coated with poly-L-lysine (Sigma Co.). After adherence, cells were post-fixed with a solution of osmium tetroxide containing 0.8–1% of potassium ferrocyanide for 30 min. Cells were subsequently dehydrated in the presence of increasing concentrations of ethanol (30%, 50%, 70%, 90%, and 100%) during 15 min each step, and then subjected to the critical point, metallized with gold and analyzed in a JEOL JSM-6390LV scanning electron microscope. The same procedure was performed for TEM in infected macrophages treated with compound **6d**.

4.11. Toxicity in mice

Female BALB/c mice (6–8 weeks old; $n = 3$ /group) were orally treated with oxadiazole **6d** at doses of 100, 50 and 25 mg/kg. Animals were monitored for signs of general toxicity, including behavior and feeding, until 24 h after treatment. Heparinized blood samples were collected after 24 h of treatment, centrifuged for 3 min. to separate out from cells and then serum components were analyzed using Analyst[®] (Hemagen, Columbia, USA) platform system.

4.12. Infection in mice

Female BALB/c mice (6–8 weeks old) were infected with bloodstream trypomastigotes by intraperitoneal inoculation of 10^4 parasites in 100 µL of saline solution and then mice were divided in groups (six animals per group). After the day 5 of infection, treatment with 50 mg/kg weight of drugs **6c** and **6d** was given orally for five consecutive days. For the control group, Benznidazole was given orally at dose of 100 mg/kg weight. Animal infection was monitored daily by counting the number of motile parasites in 5 µL of fresh blood sample drawn from the lateral tail veins as recommended by standard protocols.³³

4.13. Statistical analyses

To determine the statistical significance of each group in the in vitro/in vivo experiments, the one-way ANOVA test and the Bonferroni for multiple comparisons were used. A p value <0.05 was considered of statistical significance. The data are representative of at least two or three experiments ran in triplicate.

Acknowledgements

J.M.S.F. thanks Universität Bremen for recording NMR, MS, and HRMS. C.A.S. and M.B.P.S. thank CNPq for the fellowship, while D.R.M.M. thanks FAPESB for a scholarship. C.A.S. is also thankful to the Instituto de Física de São Carlos (University of Sao Paulo, Brazil) for allowing the use of KappaCCD diffractometer. This work received funding by Universidade Federal de Pernambuco (UFPE), Conselho Nacional de Pesquisas Brasileira (CNPq, grant 478454/2010-4), and Fundação de Amparo as Pesquisas do Estado da Bahia (FAPESB, grant 6596).

Supplementary data

Supplementary data associated with this article can be found, in the online version, at <http://dx.doi.org/10.1016/j.bmc.2012.08.047>. These data include MOL files and InChiKeys of the most important compounds described in this article.

References and notes

1. Coura, J. R.; de Castro, S. L. *Mem. Inst. Oswaldo Cruz* **2002**, *97*, 3.
2. Dias, J. C. *Mem. Inst. Oswaldo Cruz* **2009**, *104*, 41.
3. Urbina, J. A. *Acta Tropica* **2010**, *115*, 55.
4. Olivieri, B. P.; Molina, J. T.; de Castro, S. L.; Pereira, M. C.; Calvet, C. M.; Urbina, J. A.; Araújo-Jorge, T. C. *Int. J. Antimicrob. Agents* **2010**, *36*, 79.
5. McKerrow, J. H.; Sun, E.; Rosenthal, P. J.; Bouvier, J. *Annu. Rev. Microbiol.* **1993**, *47*, 821.
6. Brinen, L. S.; Hansell, E.; Cheng, J.; Roush, W. R.; McKerrow, J. H.; Fletterick, R. J. *Structure* **2000**, *8*, 831.
7. Doyle, P. S.; Zhou, Y. M.; Hsieh, I.; Greenbaum, D. C.; McKerrow, J. H.; Engel, J. C. *Plos Pathog.* **2011**, *7*, e1002139.
8. Kerr, I. D.; Lee, J. H.; Farady, C. J.; Marion, R.; Rickert, M.; Sajid, M.; Pandey, K. C.; Caffrey, C. R.; Legac, J.; Hansell, E.; McKerrow, J. H.; Craik, C. S.; Rosenthal, P. J.; Brinen, L. S. *J. Biol. Chem.* **2009**, *284*, 25697.
9. Engel, J. C.; Doyle, P. S.; McKerrow, J. H. *J. Exp. Med.* **1998**, *188*, 725.
10. Barr, S. C.; Warner, K. L.; Kornreic, B. G.; Piscitelli, J.; Wolfe, A.; Benet, L.; McKerrow, J. H. *Antimicrob. Agents Chemother.* **2005**, *49*, 5160.
11. Brak, K.; Doyle, P. S.; McKerrow, J. H.; Ellman, J. A. *J. Am. Chem. Soc.* **2008**, *130*, 6404.
12. Brak, K.; Kerr, I. D.; Barrett, K. T.; Fuchi, N.; Debnath, M.; Ang, K.; Engel, J. C.; McKerrow, J. H.; Doyle, P. S.; Brinen, L. S.; Ellman, J. A. *J. Med. Chem.* **2010**, *53*, 1763.
13. Boström, J.; Hogner, A.; Llinas, A.; Wellner, E.; Plowright, A. T. *J. Med. Chem.* **2012**, *55*, 1817.
14. Warmus, J. S.; Flamme, C.; Zhang, L. Y.; Barrett, S.; Bridges, A.; Chen, H.; Gowan, R.; Kaufman, M.; Sebolt-Leopold, J.; Leopold, W.; Merriman, R.; Ohren, J.; Pavlovsky, A.; Przybranowski, S.; Tecle, H.; Valik, H.; Whitehead, C.; Zhang, E. *Bioorg. Med. Chem. Lett.* **2008**, *18*, 6171.
15. Cottrell, D. M.; Capers, J.; Salem, M. M.; DeLuca-Fradley, K.; Croft, S. L.; Werbovetz, K. A. *Bioorg. Med. Chem.* **2004**, *12*, 2815.
16. Cerecetto, H.; Maio, R. D.; González, M.; Risso, M.; Saenz, P.; Seoane, G.; Denicola, A.; Peluffo, G.; Quijano, C.; Olea-Azar, C. *J. Med. Chem.* **1999**, *42*, 1945.
17. Steert, K.; Berg, M.; Mottram, J. C.; Westrop, G. D.; Coombs, G. H.; Cos, P.; Maes, L.; Joossens, J.; Van der Veken, P.; Haemers, A.; Augustyns, K. *ChemMedChem* **2010**, *5*, 1734.
18. Ferreira, R. F.; Bryant, C.; Ang, K. K. H.; McKerrow, J. H.; Shoichet, B. K.; Renslo, A. R. *J. Med. Chem.* **2009**, *52*, 5005.
19. Ishii, M.; Jorge, S. D.; de Oliveira, A. A.; Palace-Berl, F.; Sonehara, I. Y.; Pasqualoto, K. F.; Tavares, L. C. *Bioorg. Med. Chem.* **2011**, *19*, 6292.
20. Dürüst, Y.; Karakus, H.; Kaiser, M.; Tasdemir, D. *Eur. J. Med. Chem.* **2012**, *48*, 296.
21. Dos Santos Filho, J. M.; Leite, A. C. L.; de Oliveira, B. G.; Moreira, D. R. M.; Lima, M. S.; Soares, M. B. P.; Leite, L. F. C. *Bioorg. Med. Chem.* **2009**, *17*, 6682.
22. Fraga, C. A. M.; Barreiro, E. J. *Curr. Med. Chem.* **2005**, *12*, 23.
23. Lima, P. C.; Lima, L. M.; da Silva, K. C. M.; Léda, P. H.; de Miranda, A. L.; Fraga, C. A. M.; Barreiro, E. J. *Eur. J. Med. Chem.* **2000**, *35*, 187.
24. Fraga, C. A. M.; Barreiro, E. J. *Curr. Med. Chem.* **2006**, *13*, 167.
25. Dos Santos Filho, J. M.; Lima, J. G.; Leite, L. F. C. C. *J. Heterocycl. Chem.* **2009**, *46*, 722.
26. Dos Santos Filho, J. M.; Lima, J. G.; Leite, L. F. C. C.; Silva, J. P.; Pitta, I. R. *Heterocycl. Commun.* **2005**, *11*, 29.
27. Maldonado, C. R.; Marin, C.; Olmo, F.; Huertas, O.; Quirós, M.; Sánchez-Moreno, M.; Rosales, M. J.; Salas, J. M. *J. Med. Chem.* **2010**, *53*, 6964.
28. Soares, M. B. P.; Silva, C. V.; Bastos, T. M.; Guimarães, E. T.; Figueira, C. P.; Smirlis, D.; Azevedo-Jr, W. F. *Acta Tropica* **2012**, *112*, 224.
29. Matsuo, A. L.; Silva, L. S.; Torrecilhas, A. C.; Pascoalino, B. S.; Ramos, T. C.; Rodrigues, E. G.; Schenkman, S.; Caires, A. C.; Travassos, L. R. *Antimicrob. Agents Chemother.* **2010**, *54*, 3318.
30. Ifa, D. R.; Rodrigues, C. R.; Alencastro, R. B.; Barreiro, E. J. *Mol. Struct.* **2000**, *505*, 11.
31. Engel, J. C.; Doyle, P. S.; Palmer, J.; Hsieh, I.; Bainton, D. F.; McKerrow, J. H. *J. Cell Sci.* **1998**, *111*, 597.
32. Vannier-Santos, M. A.; de Castro, S. L. *Curr. Drug Targets* **2009**, *10*, 246.
33. Romanha, A. J.; Castro, S. L.; Soeiro, M. N.; Lannes-Vieira, J.; Ribeiro, I.; Talvani, A.; Bourdin, B.; Blum, B.; Olivieri, B.; Zani, C.; Spadafora, C.; Chiari, E.; Chatelain, E.; Chaves, G.; Calzada, J. E.; Bustamante, J. M.; Freitas-Jr, L. H.; Romero, L. I.; Bahia, M. T.; Lotrowska, M.; Soares, M.; Andrade, S. G.; Armstrong, T.; Degrave, W.; Andrade, Z. A. *Mem. Inst. Oswaldo Cruz* **2010**, *105*, 233.
34. Bettiol, E.; Samanovic, M.; Murkin, A. S.; Raper, J.; Buckner, F.; Rodriguez, A. *Plos Negl. Trop. Dis.* **2009**, *3*, e384.
35. Caffrey, C. R.; Schanz, M.; Nkemngu, N. J.; Brush, M.; Hansell, E.; Cohen, F. E.; Flaherty, T. M.; McKerrow, J. H.; Steverding, D. *Int. J. Antimicrob. Agents* **2002**, *19*, 227.
36. Carvalho, S. A.; Lopes, F. A.; Salomão, K.; Romeiro, N. C.; Wardell, S. M.; de Castro, S. L.; da Silva, E. F.; Fraga, C. A. M. *Bioorg. Med. Chem.* **2008**, *16*, 413.
37. Carvalho, S. A.; Feitosa, L. O.; Soares, M.; Costa, T. E.; Henriques, M. G.; Salomão, K.; de Castro, S. L.; Kaiser, M.; Brun, R.; Wardell, J. L.; Wardell, S. M.; Trossini, G. H.; Andricopulo, A. D.; da Silva, E. F.; Fraga, C. A. M. *Eur. J. Med. Chem.* **2012**, *54*, 512.
38. Salomão, K.; de Souza, E. M.; Carvalho, S. A.; da Silva, E. F.; Fraga, C. A. M.; Barbosa, H. S.; de Castro, S. L. *Antimicrob. Agents Chemother.* **2010**, *54*, 2023.
39. Moreira, D. R. M.; Leite, A. C. L.; Santos, R. R.; Soares, M. B. P. *Curr. Drug Targets* **2009**, *10*, 212.